CT Angiography of the Renal Arteries

13

Terri Jo Vrtiska

Abstract

Imaging of the renal arteries using noninvasive tools such as high resolution CT angiography (CTA) has largely replaced catheter angiography in the assessment of a variety of clinical indications including depicting renal donor anatomic variation, assessing renal luminal abnormalities and demonstrating complex postoperative reconstructions. This chapter reviews the indications, techniques and applications for renal arterial CTA as well as presents future directions for state-of-the-art CT scanners and processing techniques.

Keywords

Renal • Arterial • Computed tomography • CTA

Indications for Renal Arterial CT Angiography

During the past decade, CT Angiography (CTA) has become a standard noninvasive imaging modality for presentation of renal vascular anatomy and pathology. CTA has evolved from relatively slow acquisitions by single spiral scanners to rapid acquisitions by 64, 128 and 256-multichannel CT systems. In most practices, advanced imaging techniques, such as CTA, have largely replaced catheter angiography in the majority of diagnostic renal arterial studies [1]. The continued evolution of these imaging techniques provides an extremely accurate, time-efficient, and cost-effective diagnostic evaluation for medical management of renal arterial disease as well as creating a precise roadmap prior to surgical intervention. High-resolution CTA images are obtained for a variety of indications. For example, a hypertensive individual may undergo renal CTA to exclude renal artery stenosis, fibromuscular dysplasia or dissection. Tailored renal CTA examination for specific pathology might include determining if vasculitis involves the renal arteries or the extent of renal aneurysmal changes. Preoperative renal CTA planning can be useful for nephron-sparing surgery prior to resection of renal masses or as post-procedural follow-up of renal stenting or surgical revascularization. In addition, CT protocols can be augmented with

T.J. Vrtiska, MD
Department of Radiology,
Mayo Clinic College of Medicine,
200 First Street SW, Rochester, MN 55905, USA
e-mail: vrtiska.terri@mayo.edu

L.O. Lerman, S.C. Textor (eds.), *Renal Vascular Disease*,
DOI 10.1007/978-1-4471-2810-6_13,

supplemental acquisitions for evaluation of the renal parenchyma, opacification of the urinary collecting systems or depicting extrarenal pathology without the administration of additional iodinated contrast material. Appropriate tailoring of these imaging sequences can be made with only a minimal increase in acquisition time and optimization of the study for the smallest possible radiation dose to an individual patient.

Optimization of Renal Arterial CTA Acquisitions

Continued evolution of CT equipment has allowed arterial vasculature to be imaged in exquisite detail by combining high resolution (sub-millimeter) increments with rapid (sub-second) acquisition timing. Optimal acquisition parameters are required to accurately depict the main renal arteries and segmental artery branches including attention to IV contrast injection, bolus timing and acquisition technique. Adequate intravenous access is essential for optimal opacification and depiction of the renal arteries. Typically, a 20 gauge or larger IV catheter is placed in the antecubital or forearm veins of either upper extremity allowing IV contrast rates of 4–5 cc/s using a power injector. A typical renal CTA bolus is 100- to 125-mL of nonionic iodinated contrast material with a concentration of 300–370 mg/mL. A dual-headed injector allows the iodinated contrast material bolus to be followed by an IV flush of 30 cc of normal saline clearing contrast material from the upper extremity veins which maximizes contrast utilization. The amount of contrast material can be modified based on patient weight and renal function. The CTA can be acquired automatically at a fixed interval of 15–25 s or more commonly is obtained using automated bolus-tracking techniques with a region of interest placed in the abdominal aorta triggering the scan acquisition when it reaches a preset level of density, typically 100–140 Hounsfield units (HU).

Adequate anatomic coverage is critical for acquisition of optimal renal CTAs, most commonly extending from the celiac artery to the distal common iliac arteries including accessory renal arteries arising from the lower abdominal aorta (Fig. 13.1) or the common iliac arteries. In patients with suspected anatomic variation such as horseshoe kidney (Fig. 13.2), pelvic kidney (Fig. 13.3), crossed-fused renal ectopia or renal transplantation, extended coverage into the entire pelvis is preferred. Acquisition and reconstruction parameters vary but ideal slice thickness of 1–1.5 mm should be obtained with a 50 % overlap in order to create optimal 3D postprocessing. Additional 2–2.5 mm axial and coronal reconstructions can be created from the original dataset for diagnostic image review and interpretation.

Fig. 13.1 Volume rendered computed tomography angiogram (CTA) of the renal arteries with an accessory renal artery (*arrowhead*) arising from the lower abdominal aorta near the aortic bifurcation

Supplementary imaging sequences can be acquired during the CT acquisition as appropriate for the clinical indication. For example, calculi are optimally visualized on precontrast CT images and precontrast HU measurements are useful in determination of enhancement characteristics of renal masses. Delayed venous phase imaging at 70–80 s can be considered for evaluation of renal vein anatomy, renal parenchymal abnormalities and renal perfusion characteristics. Excretory phase imaging can be added to the CTA exam for a one-stop combined evaluation of renal vasculature, renal parenchyma and urothelium.

Fig. 13.2 Volume rendered CTA of a horseshoe kidney supplied by three renal arteries (*arrowheads*). The inferior mesenteric artery is noted with an *

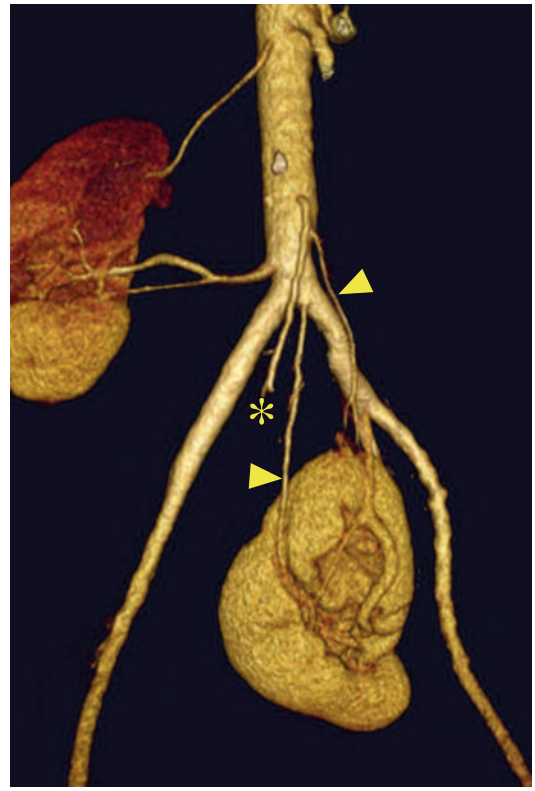

Fig. 13.3 Volume rendered CTA including a normally positioned right kidney supplied by two renal arteries and a pelvic kidney also supplied by two renal arteries (*arrowheads*). The inferior mesenteric artery is denoted by an *

Careful attention to radiation dose should be reviewed with the CT technologist performing the examination including limiting longitudinal craniocaudal coverage to the appropriate acquisition length. For example, overscanning into the chest or lower pelvis increases unnecessary radiation dose to radiosensitive structures such as the breasts or gonadal tissue. Acquiring precontrast acquisition using lower dose techniques and thicker sections (3–5 mm) also decreases the overall radiation dose. Application of mA modulation, auto-kV utilization as well as noise reduction computer algorithms are additional techniques that allow optimal visualization of the renal arteries at the lowest radiation dose.

Comparison to Other Modalities

The ability to acquire exams with increased spatial resolution and faster exam times provides the key benefits of CTA when compared to MR angiography (MRA). Depicting the extent of atheromatous calcification, which cannot be demonstrated on MRA, is another advantage. However, MRA can be obtained without radiation exposure or iodinated contrast material thus providing an optimum imaging alternative in pregnant patients as well as patients with severe iodinated contrast allergy or decreased renal function. CTA does require radiation exposure for image acquisition; however, the accuracy is less operator-dependent and especially useful in patients with a large body habitus when compared to ultrasound. The gold standard for arterial diagnostic evaluations has traditionally been invasive catheter-directed angiograms; however, cross-sectional techniques (CTA and MRA) have largely replaced the necessity for an invasive diagnostic examination (Table 13.1).

Table 13.1 Comparisons of renal arterial computed tomography angiography, magnetic resonance angiography, ultrasound and catheter angiography

	CTA	MRA	US	Cath angio
Radiation	Yes	No	No	Yes
Resolution	Isotropic	Near-isotropic	NA	4 1p/mm
Iodinated contrast	Yes	No	No	Yes
Operator dependence	No	No	Yes	Yes
Resistive indices	No	No	Yes	No
Pressure gradients	No	No	No	Yes
Total exam time (est)	5–10 s	15–20 s	20–30 min	20–30 min
Invasiveness	No	No	No	Yes
3D post-processing	Yes	Yes, automated	No	No
Contraindications (relative and absolute)	Severe contrast allergy	Pacemaker, claustrophobia, some aneurysm clips and implanted devices	None	Severe contrast allergy

Display of Variant Anatomy and Pathology with Multiplanar 2D and 3D Reconstructions

Using current computer technology, the acquired CT exam volume of data can be easily reviewed on a workstation in the traditional axial plane as well as oblique, coronal and sagittal planes maintaining isotropic display in the x, y and z axes using modern 64 channel and greater CT scanners. 3D rendering techniques such as volume-rendered (VR), curved multi-planar reconstruction (MPR) and maximum-intensity-projection (MIP) can be used by the radiologist to clarify anatomic relationships and the extent of pathologic changes. The post processed 2D and 3D images can be provided to clinicians in order to succinctly demonstrate important diagnostic information and provide educational information to patients.

Renal Donor Evaluation

Renal transplantation is currently an optimal treatment choice for end-stage renal disease. In the past, combinations of imaging exams were often used in the preoperative assessment of living renal donors including invasive catheter angiogram combined with intravenous urography. The large flank incision used for harvesting of the donated kidney provided direct visualization of the renal arterial and venous vasculature. Currently, renal donor harvesting is typically performed laparoscopically necessitating a careful preoperative roadmap of the renal vasculature. Fortunately, advances in CTA provide an accurate and complete evaluation of the donated kidney by combining visualization of the renal arteries, renal veins and urographic images into one diagnostic CT exam. Multiphase imaging techniques have been commonly used in the evaluation of renal donors including precontrast, angiographic, venographic and excretory phase imaging. However, newer techniques such as combined angiographic and excretory phase imaging [2] provide accurate imaging details of the renal vasculature while significantly decreasing radiation dose. When correlated with catheter angiography or intraoperative findings, CTA has demonstrated high sensitivity and accuracy of 95–99 % in determination of the arterial number and branching pattern as well as venous variants [3–5]. Important renal donor CT information includes:

1. Renal arterial branching pattern with a prehilar branching pattern described as less than 15–20 mm (Fig. 13.4)
2. Number of renal arteries and veins with accessory renal arteries occurring in 25–28 % of patients [3, 4, 6]
3. Anomalous renal artery and/or venous anatomy including circumaortic or retroaortic left renal veins
4. Renal parenchymal and extrarenal abnormalities including renal cell carcinoma or chronic atrophic pyelonephritis.

The arterial and venous phase images are commonly sent to post-processing workstations

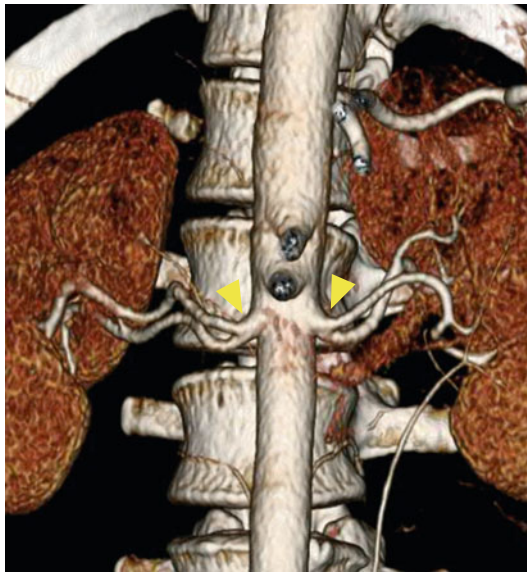

Fig. 13.4 Volume rendered CTA for a preoperative renal donor examination demonstrates early bifurcation (<10 mm) of the renal arteries bilaterally (*arrowheads*)

to reconstruct tailored 3D imaging sets, which maximally demonstrate renal anatomy and anatomic variants. Efficient processing times and dedicated protocols allow the individualized images to be made rapidly available to the referring physicians to provide preoperative planning details. In addition, the intuitive display of the 3D CTA images during the patient-physician discussions help provide instructive details to the patient regarding surgical approaches.

Renal Arterial Atherosclerotic Ostial Stenosis

Some patients undergoing CTAs of the renal arteries may be hypertensive and this noninvasive evaluation is performed to exclude an underlying treatable cause. While an anatomic cause only occurs in a few percent of patients with hypertension, atherosclerotic renal artery stenosis is the culprit in 90 % of these patients [7] with progressive disease to occlusive changes in 3–16 % [7]. Typical changes of renal arterial atheromatous stenosis involve the renal ostia and proximal 10–20 mm of the renal artery and may include mural thrombus, calcification, ulceration and post-stenotic dilatation (Fig. 13.5a–c). While there remains debate regarding the unqualified imaging method of choice for hemodynamically significant renal artery stenosis either due to atheromatous disease or fibromuscular dysplasia, CTA has demonstrated high sensitivity and specificity (92–94 %, 93–99 %) [8, 9] with a more recent study of 50 consecutive patients documenting sensitivity of 100 %, specificity of 98 % and accuracy of 98 % [10] when compared with digital subtraction angiography. CTA is also a useful guide for preprocedural planning in determination of the length of the stenotic segment, sizing criteria for balloon dilatation or stent placement and branching patterns. Current treatment of renal artery stenosis with renal artery stenting has been shown to be superior to percutaneous transluminal angioplasty alone [11] with longer patency rates. Complications of renal artery stent placement include development of in-stent restenosis from intimal hyperplasia in 17–21 % of patients [12, 13]. Follow-up of renal arterial stent placement can be performed with excellent diagnostic accuracy for detection of significant in-stent stenosis (>50 %) using new 64-detector CTA techniques including sensitivity of 100 %, specificity of 99 %, negative predictive value of 100 % and positive predictive value of 90 % [13] when compared to catheter angiography. In addition, current CTA acquisition parameters allow exams to be performed at approximately 50 % of the radiation exposure used in early CTA exams [12].

In addition to the evaluation of the renal arterial luminal changes, CTA provides a detailed evaluation of the renal parenchyma including associated focal scarring or global parenchymal loss. Careful review of the diagnostic CT images may also demonstrate an alternate secondary cause for hypertension such as an adrenal mass (aldosteronoma, pheochromocytoma (Fig. 13.6a, b), aortic coarctation or renal mass.

Fibromuscular Dysplasia

Advances in CT technology with high resolution techniques have improved visualization of more subtle renal arterial intimal abnormalities

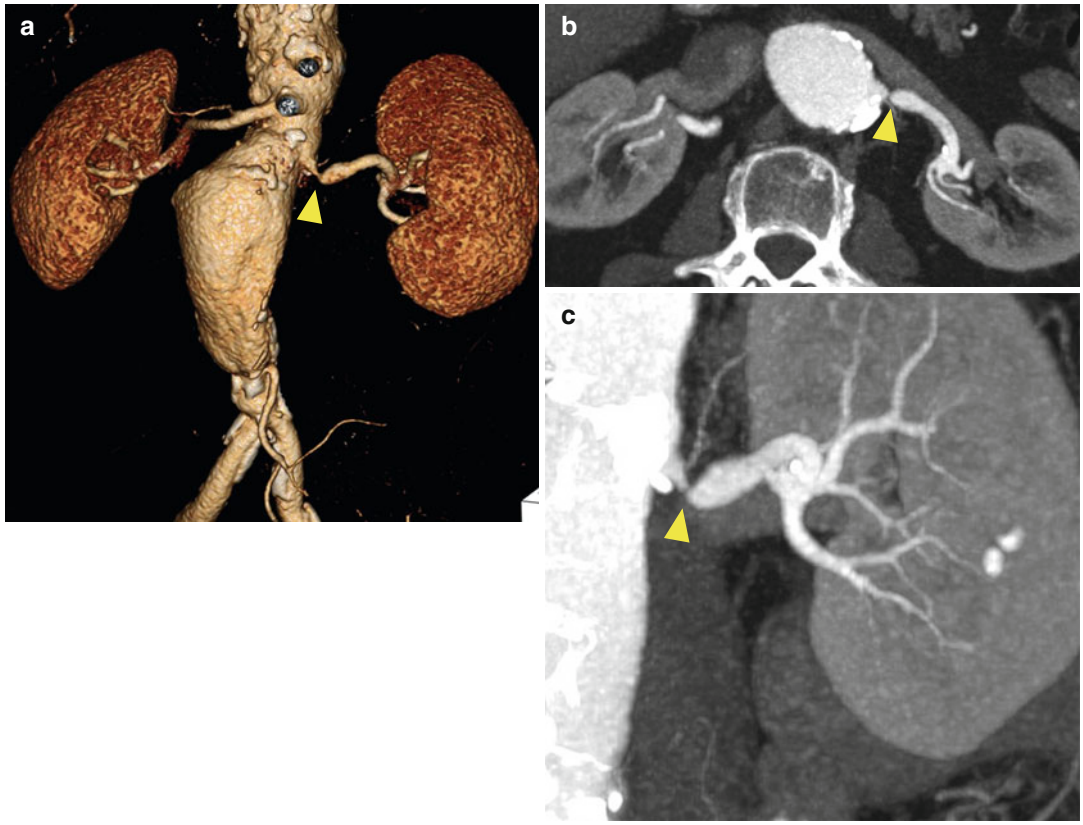

Fig. 13.5 (**a**) Volume rendered CTA demonstrated a high grade short segment stenosis just beyond the origin of the left renal artery (*arrowhead*). (**b**) Axial imaging demonstrates the high grade stenosis (*arrowhead*) with mild poststenotic dilatation. (**c**) Coronal imaging also demonstrates the focal stenosis (*arrowhead*) with mild poststenotic dilatation

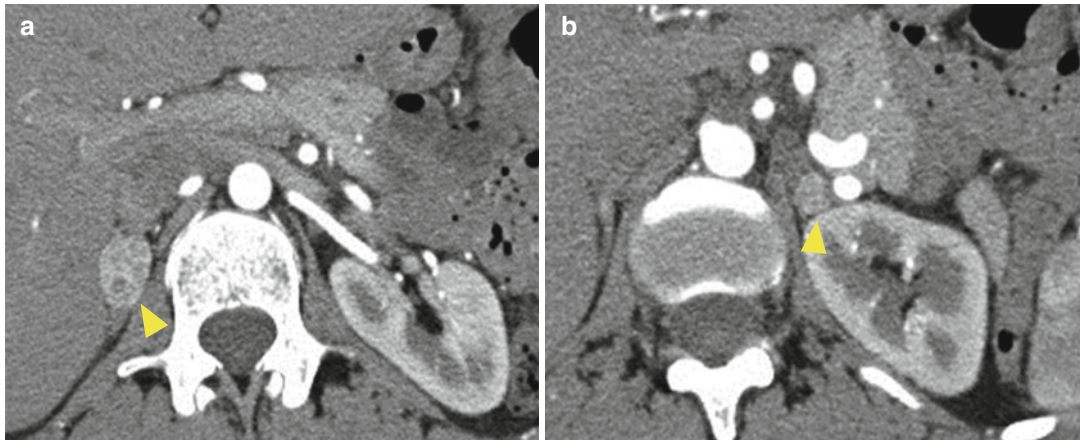

Fig. 13.6 (**a**, **b**) Axial CT images in a 45 year old female with hypertension and a history of Neurofibromatosis type 1. A hypervascular nodule in the right and left adrenal glands (*arrowheads*) were surgically removed and pathologically confirmed as bilateral pheochromocytomas

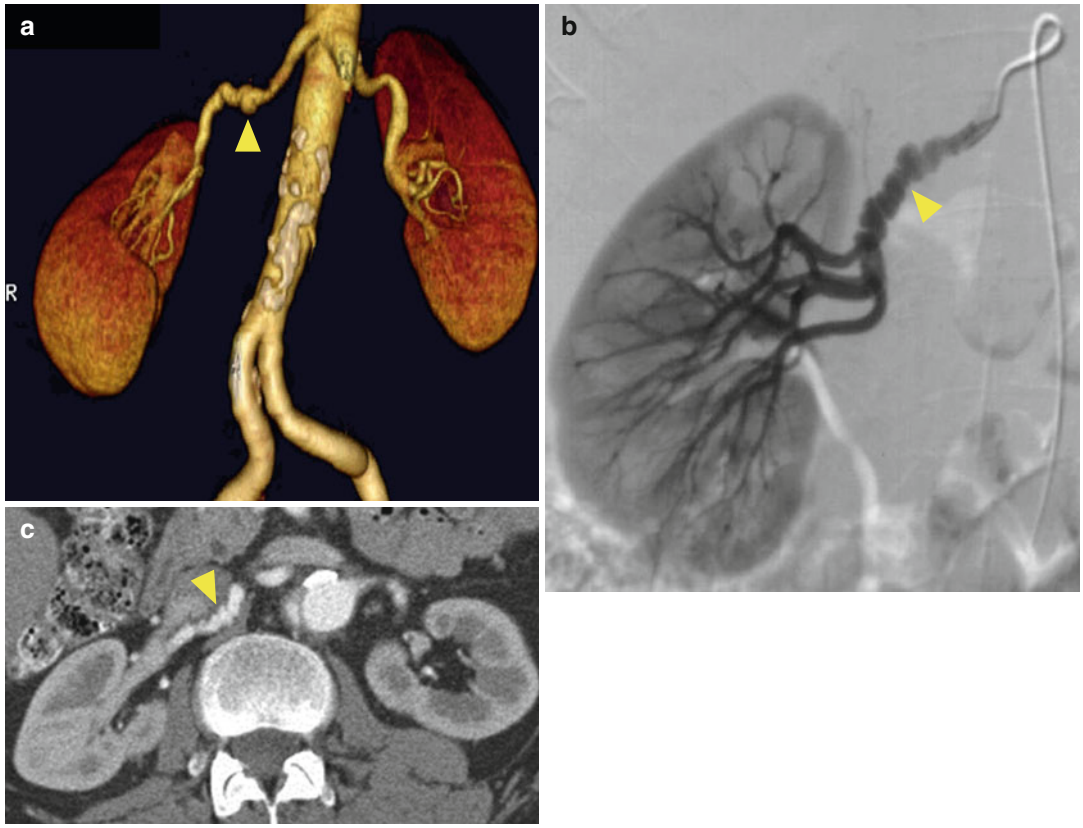

Fig. 13.7 (**a**) Volume rendered CTA demonstrating a classic "string of pearls" consistent with fibromuscular dysplasia (FMD) (*arrowhead*) in the right renal artery. (**b**) Catheter angiogram confirmation of FMD in the same patient (*arrowhead*). (**c**) Axial CT source images demonstrating typical changes of FMD in the mid main right renal artery (*arrowhead*)

such as fibromuscular dysplasia (FMD). Initial publications [14] using early CT technology reliably detected renal artery FMD, but did not advocate for replacement of catheter-directed angiograms. Subsequent publication demonstrated 100 % detection rate of renal arterial FMD by CTA [15] when compared to catheter angiography. Current state-of-the-art CT scanners provide improved spatial resolution compared to earlier exams with accuracy in detection of FMD equivalent or slightly superior to MR angiography [16, 17]; however, both of these technologies are continually evolving.

While renal artery stenosis is most commonly due to atheromatous disease, the majority of the remaining 10–20 % of stenotic renal arteries is due to renal artery FMD [18, 19]. The prevalence of FMD in the general population is rare but has been estimated at nearly 4 % [20] with a 3:1 predominance of females to males, most commonly in the 30–50 year old age group. FMD is divided into subtypes based on the involved layer of the arterial wall (intima, media or adventitia) [21]. Medial FMD is the most common resulting in the classic "string of pearls" appearance both on catheter angiography and CTA. Intimal FMD and adventitial fibroplasia are less common and cannot be separated into distinct subtypes by CTA but can be suspected with tubular segments of stenosis. Involvement of more than one arterial wall layer also occurs pathologically.

The findings of FMD on CTA include most commonly the beaded or string of pearls characteristics (Fig. 13.7a–c) which can be associated with more focal aneurysmal disease. Additional findings on CTA include an arterial

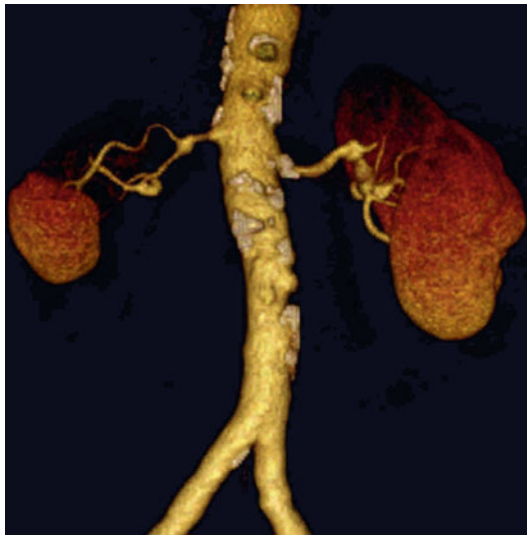

Fig. 13.8 Volume rendered CTA demonstrates severe long tubular stenoses in the right renal artery consistent with a variant of FMD typically arising from pathologic changes in the intima or adventitia

segment of long smooth narrowing, unifocal band-like stenosis or tubular stenosis (Fig. 13.8). Unlike proximal atheromatous changes of the renal artery, FMD is most common in the mid to distal main renal arteries but can extend into the first division branches. Bilateral disease occurs in 60 % of cases [21]. Complications of FMD can also be depicted on CTA including dissection, occlusion or thrombosis.

An additional rare, noninflammatory disease which most commonly involves the visceral arteries including the renal arteries is segmental arterial mediolysis (SAM) which affects the small to medium arterial distribution and has equal distribution between men and women. Some authors consider SAM to be a variant of or precursor to FMD [22–25]. The average age of presentation is in the fifth decade of life. The etiology of this disorder is unknown and lack of familiarity with the imaging findings can result in misdiagnosis of vasculitis or even neoplasm. CTA has been shown to be a useful imaging tool in the diagnosis and follow-up of patients with SAM [24]. Patients most commonly present with abdominal, flank or chest pain and may be hypertensive or have hematuria. Findings of SAM include dissections, aneurysms, intramural hematomas, occlusions (Fig. 13.9a, b) [25, 26] and more commonly involves the mesenteric arteries (70 %) with the renal arteries involvement in 50 % [26]. Approximately 50 % of patients progress and 50 % resolve or decrease [26].

Renal Arterial Dissection and Thrombosis

Spontaneous renal arterial dissection is a rare cause of acute flank pain in the ER setting and is often accompanied with hypertension. The dissection is thought to result from an intramural hemorrhage or entrance of blood into the arterial wall through an intimal tear [27]. Underlying risk factors for spontaneous renal arterial dissection include atheromatous disease, renal arterial aneurysm, FMD, connective tissue disease (such as Ehlers-Danlos syndrome) or extension from an aortic dissection [27]. Current CTA technology allows direct visualization of the dissected intimal flap (Fig. 13.10a, b). Additional imaging findings of a renal arterial dissection include irregular dilatation and narrowing of the opacified arterial lumen, thrombosis of a renal arterial segment and/or regions of decreased perfusion to the renal parenchyma supplied by the dissected or thrombosed renal artery. Management options include conservative observational therapy with or without anticoagulation as well as surgical or endovascular intervention.

CTA also provides accurate determination of luminal patency and presence of renal arterial perfusion abnormalities or infarction from thromboembolic disease (Fig. 13.11a, b). CTA findings include a central low attenuation thrombus/embolus within the renal artery. The thromboembolism often originates from the heart or from irregular and ulcerated thoracoabdominal atheromatous disease. Emboli to the renal arteries can also be associated with atrial fibrillation, postmyocardial infarct emboli, bacterial endocarditis or atrial myxomas. Associated renal parenchymal perfusion changes most commonly consist of wedge-shaped parenchymal defects or global decreased perfusion changes to the involved kidney.

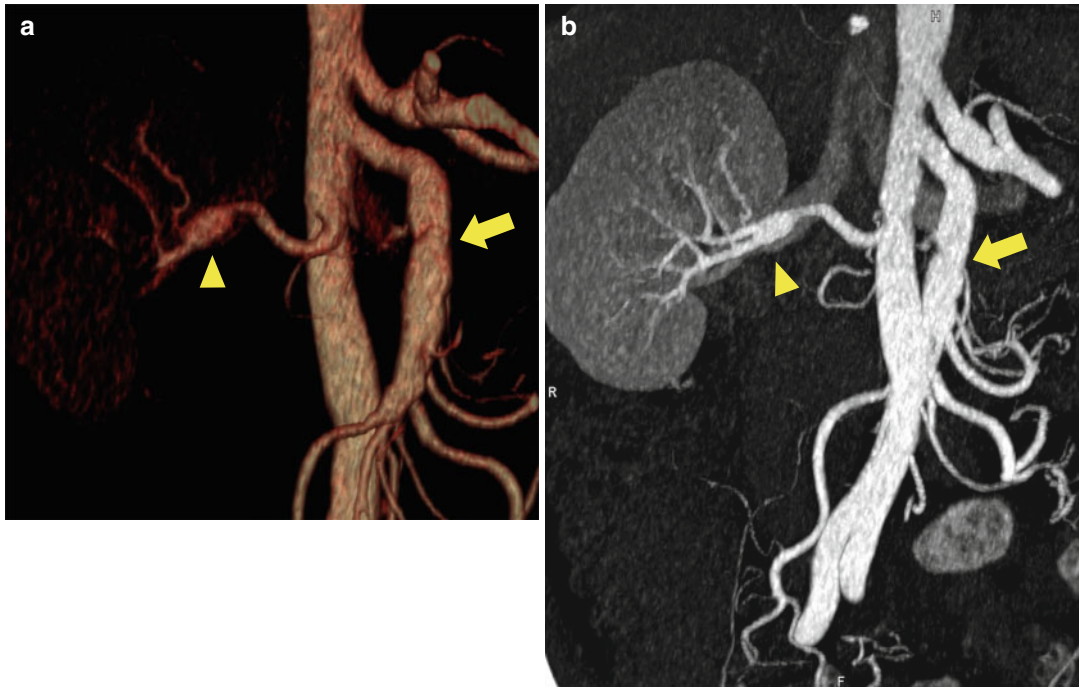

Fig. 13.9 (**a**, **b**) Volume rendered CTA (**a**) and a Maximum Intensity Projection (MIP) image (**b**) with focal aneurysmal changes in the right renal artery (*arrowhead*) and diffuse dilatation of the superior mesenteric artery (*arrow*) consistent with CTA findings of segmental arterial mediolysis (SAM)

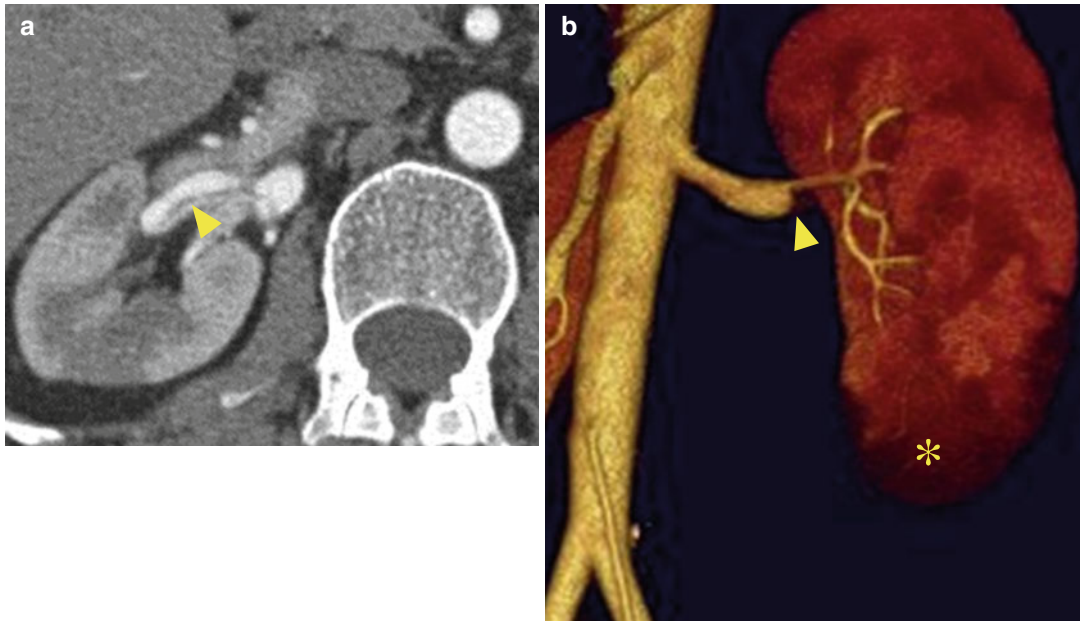

Fig. 13.10 (**a**) Axial CT image with intimal dissection extending into the anterior division of the right renal artery (*arrowhead*). (**b**) Volume rendered CTA demonstrates the abrupt occlusion from prior dissection and intramural hematoma involving the distal left renal artery. Note the decreased perfusion to the lower pole of the left kidney (*)

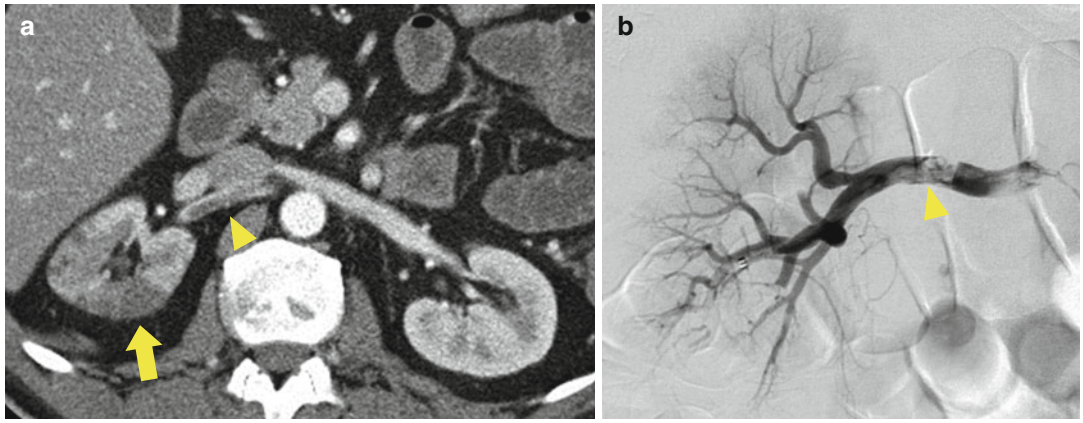

Fig. 13.11 (**a**, **b**) Axial images from a CTA (**a**) and catheter-directed renal angiogram (**b**) with focal embolus in the main right renal artery (*arrowhead*). Associate decreased parenchymal perfusion is evident in the lateral and posterior right kidney (*arrow*)

Vasculitis

Noninvasive vascular imaging such as CTA has replaced catheter angiography in the evaluation and follow-up of vasculitis given the great advantage of evaluation of both the arterial wall as well as luminal changes. Systemic vasculitides frequently involve the renal arteries. The large vessel vasculitides most commonly resulting in renal arterial abnormalities include giant cell (temporal) arteritis and Takayasu arteritis. CTA demonstrates not only the circumferential and concentric wall thickening of active inflammatory changes but also the stenosis of the renal arterial ostia either unilaterally or bilaterally (Fig. 13.12a, b). Less commonly, aneurysms and occlusions are detected. A medium vessel vasculitis involving the kidneys that has been demonstrated by CTA using the latest technological advancements is polyarteritis nodosa (PAN) [28]. Areas of decreased parenchymal perfusion and infarction are associated with renal involvement in PAN and can be confused with pyelonephritis. Multiple small intrarenal arterial aneurysms measuring 1–5 mm are occasionally demonstrated by CTA typically occurring in the intrarenal arterial distribution of the distal interlobar arteries [28]. Associated changes of the renal arteries include ectasia, occlusion and rare aneurysmal rupture [29].

Renal Arterial Aneurysm

Aneurysms uncommonly involve the renal arteries occurring in 0.1 % of the population [30]. Renal arterial aneurysms (RAAs) are more commonly seen in women and are typically solitary and unilateral (Fig. 13.13a–c). Saccular RAAs are more frequent (79 %) than the fusiform type and are most commonly located at the distal bifurcation of the main renal artery [30–32]. The fusiform type of aneurysm is commonly associated with changes of renal artery medial FMD. RAAs are commonly asymptomatic and discovered incidentally [31] but complications such as hypertension, renal infarction, rupture, renal arterial thrombosis and arteriovenous fistula do occur. Fortunately, the risk of spontaneous rupture of a RAA is very low. Specific risk factors for RAA rupture include premenopausal women, pregnancy and increasing size of the aneurysm. The largest clinical experience with RAA was described by Henke et al [31] in a retrospective evaluation of 252 RAAs over 35 years in 168 patients and used to develop recommendations for management of RAAs that were recently confirmed by Morita et al [33]. Options for RAAs intervention include aneurysmectomy, renal arterial bypass, embolization, endovascular stenting and nephrectomy.

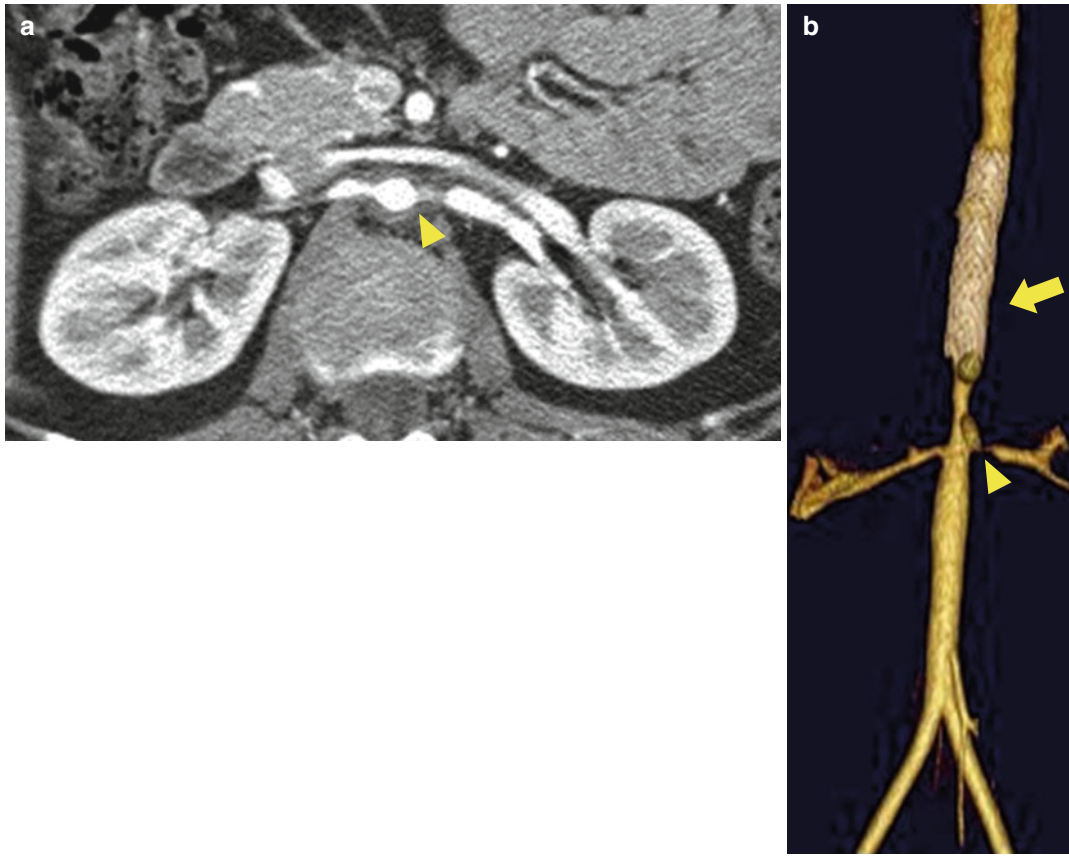

Fig. 13.12 (**a**) Axial images from a CTA demonstrates a rind of circumferential wall thickening surrounding the abdominal aorta at the level of the renal arteries consistent with vasculitis resulting in high grade stenosis at the origin of the left renal artery. (**b**) Volume rendered CTA image demonstrates the high grade stenosis at the origin of the left renal artery below a stented segment of the descending thoracic aorta (*arrow*)

Diseases most commonly associated with RAAs are hypertension and FMD [30], but RAAs also occur with segmental arterial mediolysis [26], arteritis, Marfan's syndrome, Ehlers Danlos Type IV and neurofibromatosis. An additional rare disease associated with multiple tiny renal peripheral intrarenal aneurysms is polyarteritis nodosa (Fig. 13.14a, b).

CTA is helpful to determine the size, contour and calcification of a single or multiple RAAs. In addition, CTA accurately depicts the anatomic relationship of the aneurysm to the main renal artery as well as to segmental intrarenal branches. Careful follow-up measurements and comparisons using sequential renal CTA exams exclude aneurysm enlargement or rupture and help determine the appropriate timing for endovascular or open surgical intervention.

Renal Trauma

High-grade injuries involving the renal artery occur in 11 % of traumatic injuries to the kidney [34] and are classified by the American Association of Surgeons in Trauma grading system [34, 35] as a Grade 4 injury when involving the renal artery or vein with a contained hemorrhage, whereas avulsion of the renal hilum that devascularizes the kidney is a Grade 5 injury. Renal arterial injuries include renal arterial dissection, occlusion and thrombosis (Fig. 13.15),

Fig. 13.13 (**a**–**c**) Axial images (**a**), coronal MIP image (**b**), and volume rendered 3D image (**c**) from a renal CTA demonstrates a well-circumscribed renal artery aneurysm (*arrowhead*) in the right renal hilum measuring 25 mm in diameter with minimal mural thrombus or calcification

which may be associated with perfusion changes to the involved renal parenchyma segment. Extraluminal contrast extravasation or renal arterial pseudoaneurysm are CTA findings which also denote a renal pedicle injury [36].

Nephron-Sparing Surgery/Follow-up

CTA is useful for preoperative evaluation prior to resection of renal masses such as renal cell carcinoma. Renal interventions are being performed using less invasive surgical techniques for laparoscopic removal of renal tumors. Appropriate indications for nephron-sparing surgery (NSS) have expanded beyond that of a solitary kidney, an abnormal contralateral kidney, multiple bilateral renal tumors or decreased renal function. Detection of 50 % of renal cell carcinomas are made incidentally [37] given the extensive availability and utilization of advanced cross-section imaging. By combining the earlier tumor detection and advances in NSS techniques, the indications for resection of renal masses using NSS have expanded to include the incidental, small (<4 cm) cortical renal mass (Fig. 13.16a, b) or the peripheral, exophytic mass without metastases. CTA is an important preoperative planning tool for small tumors that can be resected using these techniques by accurately depicting renal arterial and venous anatomy [38]. In addition, accurate display of the renal arterial supply of large renal tumors is determined in 98 % of cases [39] and the depiction of renal vein invasion provides a

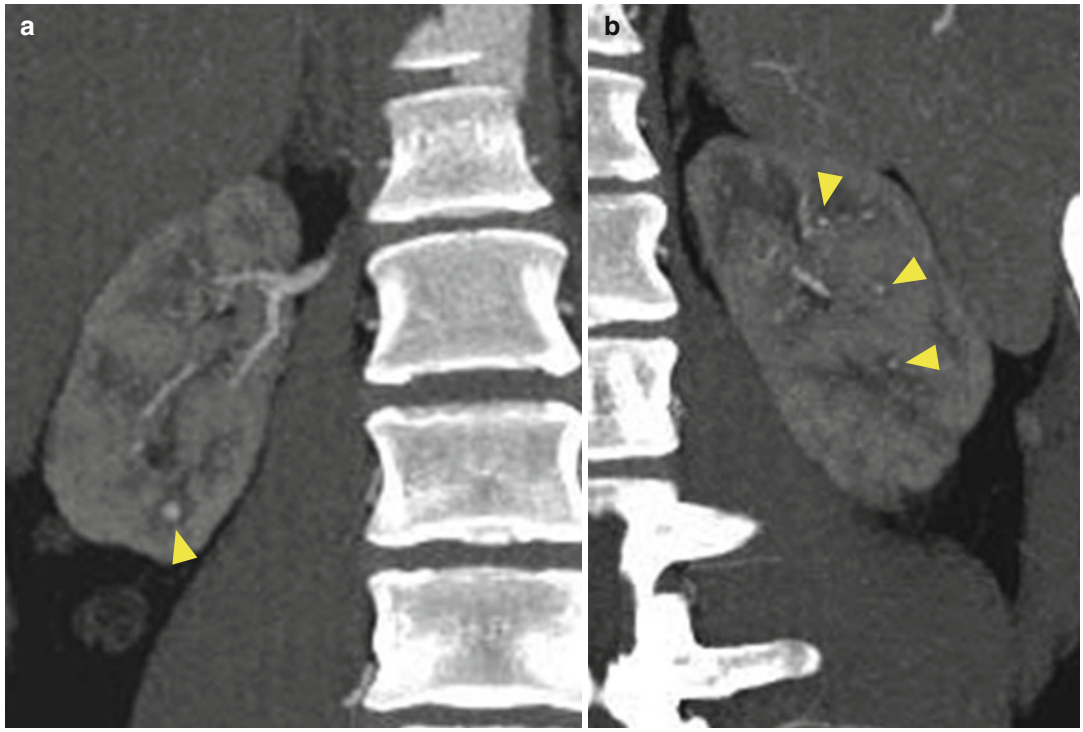

Fig. 13.14 (**a**, **b**) Coronal MIP images demonstrate multiple small peripheral intra-arterial aneurysms (*arrowheads*) consistent with polyarteritis nodosa (PAN)

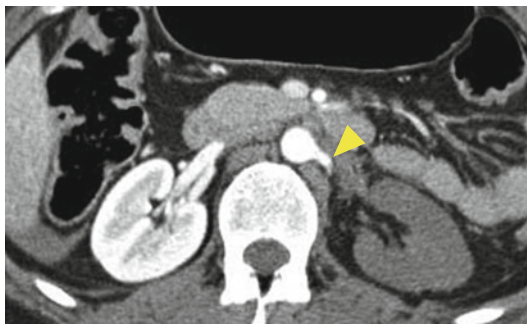

Fig. 13.15 Axial CTA images following motor vehicle accident in a 25 year old male demonstrate abrupt occlusion of the left renal artery (*arrowhead*) with lack of perfusion to the left kidney consistent with traumatic left renal artery injury

helpful preoperative planning tool with a high positive and negative predictive value by renal CTA (92 and 97 % respectively) [40]. The extent of IVC thrombus by CT is also a useful imaging planning contribution by depicting presence of tumor thrombus above the diaphragm potentially altering the surgical approach to tumor resection.

Future Opportunities in CTA of the Kidneys

Optimization of renal artery CTA in the future includes technique enhancement along with continued radiation dose reduction using both hardware and software advancements. The newest advances in CT technology include dual energy CT (DECT) acquisitions, low kV CTA and iterative reconstruction techniques, which are providing new avenues for the evaluation of renal arterial anatomy and pathology using the lowest radiation doses. With DECT, the acquisition of images at two different kilovoltages (typically 80 and 140 kVp) provides new opportunities for specific material characterization and separation of anatomic structures [41, 42]. For example, renal arterial wall atheromatous calcification could be separated from the opacified lumen with improved depiction of renal arterial stenosis such has been currently applied to calcified lower extremity arterial vasculature [43] and the carotid arteries [44]. DECT also provides for rapid

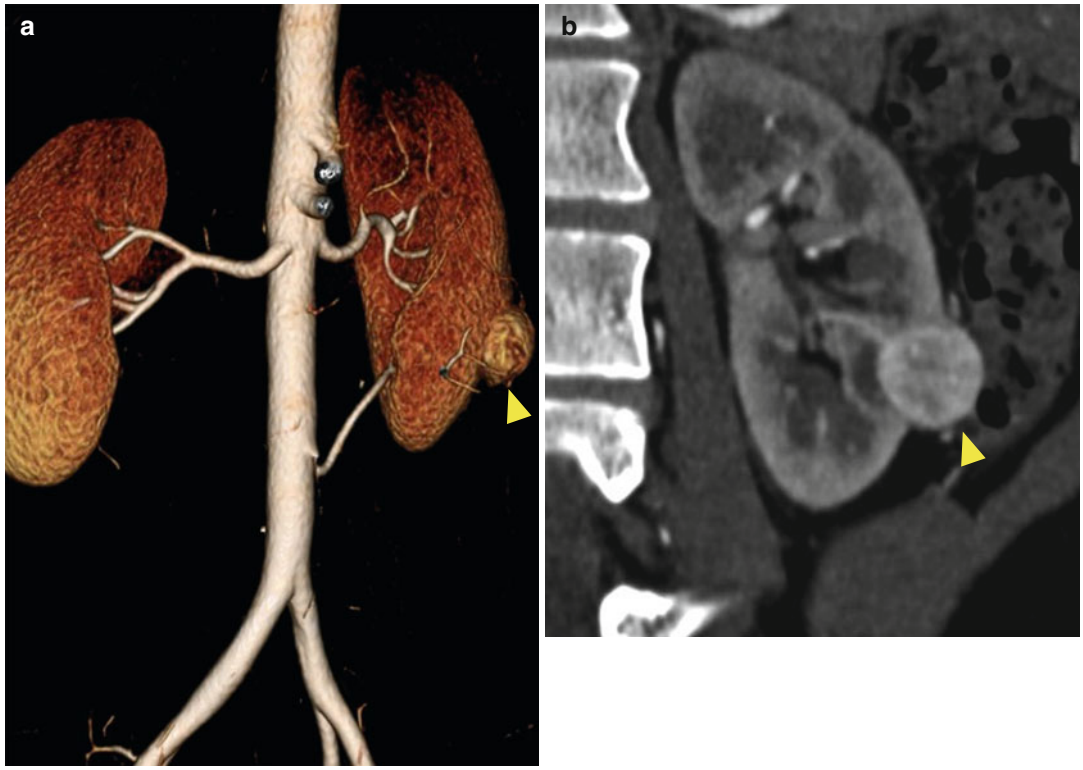

Fig. 13.16 (**a**, **b**) Volume rendered 3D CTA (**a**) and coronal reconstruction (**b**) demonstrate a 2.5 cm intensely hypervascular exophytic mass arising from the lateral lower pole of the left kidney (*arrow*) which was shown to represent a small renal cell carcinoma at surgical resection

characterization and separation of bones which enhances rendering of 3D CTA exams. In addition, virtual noncontrast CT imaging can be created from the contrast enhanced CT data for precontrast measurements of indeterminate renal masses or detection of urinary calculi [42]. Low kV CTA exams allow improved visualization of high attenuation structures such as small intrarenal arterial branches [45, 46] by taking advantage of the specific attenuation characteristics including the molecular properties (k-edge) of iodine at lower kVs. Application of low kV imaging in the appropriate (typically smaller) patients can result in reduced radiation dose as well as potential reduction in the volume of iodinated contrast material needed for a renal arterial CTA [45, 46]. Finally, while decreases in tube voltage and radiation doses are a beneficial direction in the optimal care of patients with renal arterial disease, these improvements can be negated by an increase in image noise and a decrease in image quality. Fortunately, additional advances in CT technology including reconstruction of imaging data through advanced computer algorithms termed iterative reconstruction [47] can offset the challenges of image noise and potential image quality reduction while lowering radiation dose by 50 % or greater.

Conclusion

CTA provides a highly accurate evaluation of the renal arteries. Continued advances in CT scanner acquisitions and image post-processing technologies will continue to further the accurate depiction and diagnosis of renal arterial anatomy and pathology at the lowest possible radiation dose tailored to the specific clinical need of the patient.

References

1. Glockner JF, Vrtiska TJ. Renal MR and CT angiography: current concepts. Abdom Imaging. 2007;32:407–20.
2. Zamboni GA, Romero JY, Raptopoulos VD. Combined vascular-excretory phase MDCT angiography in the preoperative evaluation of renal donors. AJR Am J Roentgenol. 2010;194:145–50.
3. Holden A, Smith A, Dukes P, Pilmore H, Yasutomi M. Assessment of 100 live potential renal donors for laparoscopic nephrectomy with multi-detector row helical CT. Radiology. 2005;237:973–80.
4. Gluecker TM, Mayr M, Schwarz J, Bilecen D, Voegele T, Steiger J, et al. Comparison of CT angiography with MR angiography in the preoperative assessment of living kidney donors. Transplantation. 2008;86:1249–56.
5. Pozniak MA, Balison DJ, Lee Jr FT, Tambeaux RH, Uehling DT, Moon TD. CT angiography of potential renal transplant donors. Radiographics. 1998;18:565–87.
6. Pollak R, Prusak BF, Mozes MF. Anatomic abnormalities of cadaver kidneys procured for purposes of transplantation. Am Surg. 1986;52:233–5.
7. Safian RD, Textor SC. Renal-artery stenosis. N Engl J Med. 2001;344:431–42.
8. Willmann JK, Wildermuth S, Pfammatter T, Roos JE, Seifert B, Hilfiker PR, et al. Aortoiliac and renal arteries: prospective intraindividual comparison of contrast-enhanced three-dimensional MR angiography and multi-detector row CT angiography. Radiology. 2003;226:798–811.
9. Rountas C, Vlychou M, Vassiou K, Liakopoulos V, Kapsalaki E, Koukoulis G, et al. Imaging modalities for renal artery stenosis in suspected renovascular hypertension: prospective intraindividual comparison of color Doppler US, CT angiography, GD-enhanced MR angiography, and digital substraction angiography. Ren Fail. 2007;29:295–302.
10. Fraioli F, Catalano C, Bertoletti L, Danti M, Fanelli F, Napoli A, et al. Multidetector-row CT angiography of renal artery stenosis in 50 consecutive patients: prospective interobserver comparison with DSA. Radiol Med. 2006;111:459–68.
11. Leertouwer TC, Gussenhoven EJ, Bosch JL, van Jaarsveld BC, van Dijk LC, Deinum J, et al. Stent placement for renal arterial stenosis: where do we stand? A meta-analysis. Radiology. 2000;216:78–85.
12. Manousaki E, Perisinakis K, Karantanas A, Tsetis D. MDCT angiography assessment of renal artery in-stent restenosis: can we reduce the radiation exposure burden? A feasibility study. Eur J Radiol. 2011;79:224–31.
13. Steinwender C, Schutzenberger W, Fellner F, Honig S, Schmitt B, Focke C, et al. 64-Detector CT angiography in renal artery stent evaluation: prospective comparison with selective catheter angiography. Radiology. 2009;252:299–305.
14. Beregi JP, Louvegny S, Gautier C, Mounier-Vehier C, Moretti A, Desmoucelle F, et al. Fibromuscular dysplasia of the renal arteries: comparison of helical CT angiography and arteriography. AJR Am J Roentgenol. 1999;172:27–34.
15. Sabharwal R, Vladica P, Coleman P. Multidetector spiral CT renal angiography in the diagnosis of renal artery fibromuscular dysplasia. Eur J Radiol. 2007;61:520–7.
16. Willoteaux S, Faivre-Pierret M, Moranne O, Lions C, Bruzzi J, Finot M, et al. Fibromuscular dysplasia of the main renal arteries: comparison of contrast-enhanced MR angiography with digital subtraction angiography. Radiology. 2006;241:922–9.
17. Vasbinder GB, Nelemans PJ, Kessels AG, Kroon AA, Maki JH, Leiner T, et al. Accuracy of computed tomographic angiography and magnetic resonance angiography for diagnosing renal artery stenosis. Ann Intern Med. 2004;141:674–82; discussion 682.
18. Youngberg SP, Sheps SG, Strong CG. Fibromuscular disease of the renal arteries. Med Clin North Am. 1977;61:623–41.
19. Liu PS, Platt JF. CT angiography of the renal circulation. Radiol Clin North Am. 2010;48:347–65, viii–ix.
20. Cragg AH, Smith TP, Thompson BH, Maroney TP, Stanson AW, Shaw GT, et al. Incidental fibromuscular dysplasia in potential renal donors: long-term clinical follow-up. Radiology. 1989;172:145–7.
21. Persu A, Touze E, Mousseaux E, Barral X, Joffre F, Plouin PF. Diagnosis and management of fibromuscular dysplasia: an expert consensus. Eur J Clin Invest. 2012;42:338–47.
22. Lie JT. Segmental mediolytic arteritis. Not an arteritis but a variant of arterial fibromuscular dysplasia. Arch Pathol Lab Med. 1992;116:238–41.
23. Slavin RE, Saeki K, Bhagavan B, Maas AE. Segmental arterial mediolysis: a precursor to fibromuscular dysplasia? Mod Pathol. 1995;8:287–94.
24. Michael M, Widmer U, Wildermuth S, Barghorn A, Duewell S, Pfammatter T. Segmental arterial mediolysis: CTA findings at presentation and follow-up. AJR Am J Roentgenol. 2006;187:1463–9.
25. Filippone EJ, Foy A, Galanis T, Pokuah M, Newman E, Lallas CD, et al. Segmental arterial mediolysis: report of 2 cases and review of the literature. Am J Kidney Dis. 2011;58:981–7.
26. Kalva SP, Somarouthu B, Jaff MR, Wicky S. Segmental arterial mediolysis: clinical and imaging features at presentation and during follow-up. J Vasc Interv Radiol. 2011;22:1380–7.
27. Stawicki SP, Rosenfeld JC, Weger N, Fields EL, Balshi JD. Spontaneous renal artery dissection: three cases and clinical algorithms. J Hum Hypertens. 2006;20:710–8.
28. Ozaki K, Miyayama S, Ushiogi Y, Matsui O. Renal involvement of polyarteritis nodosa: CT and MR findings. Abdom Imaging. 2009;34:265–70.
29. Stanson AW, Friese JL, Johnson CM, McKusick MA, Breen JF, Sabater EA, et al. Polyarteritis nodosa: spectrum of angiographic findings. Radiographics. 2001;21:151–9.

30. Stanley JC, Rhodes EL, Gewertz BL, Chang CY, Walter JF, Fry WJ. Renal artery aneurysms. Significance of macroaneurysms exclusive of dissections and fibrodysplastic mural dilations. Arch Surg. 1975;110:1327–33.
31. Henke PK, Cardneau JD, Welling 3rd TH, Upchurch Jr GR, Wakefield TW, Jacobs LA, et al. Renal artery aneurysms: a 35-year clinical experience with 252 aneurysms in 168 patients. Ann Surg. 2001;234: 454–62; discussion 62–3.
32. Eskandari MK, Resnick SA. Aneurysms of the renal artery. Semin Vasc Surg. 2005;18(4):202–8.
33. Morita K, Seki T, Iwami D, Sasaki H, Fukuzawa N, Nonomura K. Long-term outcome of single institutional experience with conservative and surgical management for renal artery aneurysm. Transplant Proc. 2012;44:1795–9.
34. Tinkoff G, Esposito TJ, Reed J, Kilgo P, Fildes J, Pasquale M, et al. American Association for the Surgery of Trauma Organ Injury Scale I: spleen, liver, and kidney, validation based on the National Trauma Data Bank. J Am Coll Surg. 2008;207:646–55.
35. Moore EE, Shackford SR, Pachter HL, McAninch JW, Browner BD, Champion HR, et al. Organ injury scaling: spleen, liver, and kidney. J Trauma. 1989;29: 1664–6.
36. Kawashima A, Sandler CM, Ernst RD, Tamm EP, Goldman SM, Fishman EK. CT evaluation of renovascular disease. Radiographics. 2000;20:1321–40.
37. Sheth S, Scatarige JC, Horton KM, Corl FM, Fishman EK. Current concepts in the diagnosis and management of renal cell carcinoma: role of multidetector ct and three-dimensional CT. Radiographics. 2001;21 Spec No:S237–54.
38. Kumar S, Neyaz Z, Gupta A. The utility of 64 channel multidetector CT angiography for evaluating the renal vascular anatomy and possible variations: a pictorial essay. Korean J Radiol. 2010;11:346–54.
39. Ferda J, Hora M, Hes O, Ferdova E, Kreuzberg B. Assessment of the kidney tumor vascular supply by two-phase MDCT-angiography. Eur J Radiol. 2007; 62:295–301.
40. Welch TJ, LeRoy AJ. Helical and electron beam CT scanning in the evaluation of renal vein involvement in patients with renal cell carcinoma. J Comput Assist Tomogr. 1997;21:467–71.
41. Graser A, Johnson TR, Chandarana H, Macari M. Dual energy CT: preliminary observations and potential clinical applications in the abdomen. Eur Radiol. 2009;19:13–23.
42. Vrtiska TJ, Takahashi N, Fletcher JG, Hartman RP, Yu L, Kawashima A. Genitourinary applications of dual-energy CT. AJR Am J Roentgenol. 2010;194: 1434–42.
43. Brockmann C, Jochum S, Sadick M, Huck K, Ziegler P, Fink C, et al. Dual-energy CT angiography in peripheral arterial occlusive disease. Cardiovasc Intervent Radiol. 2009;32:630–7.
44. Thomas C, Korn A, Ketelsen D, Danz S, Tsifikas I, Claussen CD, et al. Automatic lumen segmentation in calcified plaques: dual-energy CT versus standard reconstructions in comparison with digital subtraction angiography. AJR Am J Roentgenol. 2010;194: 1590–5.
45. Pinho DF, Kulkarni NM, Krishnaraj A, Kalva SP, Sahani DV. Initial experience with single-source dual-energy CT abdominal angiography and comparison with single-energy CT angiography: image quality, enhancement, diagnosis and radiation dose. Eur Radiol. 2012;23:351–9.
46. Cho ES, Yu JS, Ahn JH, Kim JH, Chung JJ, Lee HK, et al. CT angiography of the renal arteries: comparison of lower-tube-voltage CTA with moderate-concentration iodinated contrast material and conventional CTA. AJR Am J Roentgenol. 2012;199: 96–102.
47. Winklehner A, Karlo C, Puippe G, Schmidt B, Flohr T, Goetti R, et al. Raw data-based iterative reconstruction in body CTA: evaluation of radiation dose saving potential. Eur Radiol. 2011;21:2521–6.